

Experimental background behind new AASHTO LRFD specifications for partially debonded strands

Mathew W. Bolduc, Bahram M. Shahrooz, Kent A. Harries, Richard A. Miller, Henry G. Russell, and William A. Potter

- To develop a unified approach for the design of partially debonded strands in prestressed concrete highway bridge girders, a coordinated analytical and experimental investigation was conducted.
- The results from the testing of full-scale I- and U-shaped girders indicate that partially debonding strands does not result in deleterious performance if adequate reinforcement is provided to resist the longitudinal tension due to bending and shear.
- The requirements for debonded strands were revised significantly in the ninth edition of the AASHTO LRFD specifications based on the presented research.

In prestressed concrete bridge girder fabrication, the following four methods are commonly used to meet limits on the extreme fiber concrete tensile stress at prestress strand release:

- partial debonding of several strands near the girder end
- harping some strands
- adding top strands
- a combination of these methods

Strands that can be harped are limited to those aligned within the member webs and may be further limited by the casting bed. For some girder shapes, such as boxes, harping is not practical. The preference for partial debonding or harping to relieve extreme-fiber tensile stress varies among states.¹ Partial debonding may also be used to satisfy the American Association of State Highway and Transportation Officials' *AASHTO LRFD Bridge Design Specifications*² article 5.9.4.4.1 requirements for splitting resistance at the ends of prestressed concrete girders, which require transverse confining reinforcement sufficient to resist 4% of the total prestressing force at transfer to be located within $h/4$ of the girder end, where h is the component depth. Partial debonding reduces the prestressing force, which can potentially cause splitting at the end of the girder. In addition, partial debonding can be used to relieve the compressive stress (AASHTO LRFD Specifications article 5.9.2.3.1a) at the end region when required.

Excessive debonding, however, can reduce the flexural and shear capacity near the girder ends as the tensile resistance provided by prestressing reinforcement in the debonded region ($A_{ps}f_{ps}$, where A_{ps} is the area of prestressing steel and f_{ps} is average stress in prestressing steel at nominal flexural resistance) is reduced. The concrete component of shear strength is also reduced because the prestressing force in regions of partial debonding is smaller. Accordingly, the AASHTO LRFD specifications places limits on the amount of partial debonding.

As part of National Cooperative Highway Research Program (NCHRP) project 12-91, a comprehensive study was conducted to develop a unified approach for the design of prestressed concrete bridge girders with partially debonded strands.¹ Based on the results and recommendations of this study and previous studies,³⁻⁸ the requirements for debonded strands were revised in the ninth edition of the AASHTO LRFD specifications.² This paper summarizes the experimental component of NCHRP project 12-91 and the results that support some of these new requirements.

Experimental program

Both ends of six full-scale prestressed concrete bridge girders (12 tests) with different debonding ratios (area of debonded strands/total area of strands) were tested to failure. One end of all but one of the girders (designated as end B) had a debonding ratio of less than 25%; the remaining girder had a debonding ratio of 27%. The debonding ratio in the other end (designated as end A) was greater than 25% in all test girders. Except for the level of debonding ratio, the detailing and loading of end A and end B were identical. The performances of end A and end B were compared. The test variables were girder shape (single-web girder, box girder, or U girder), debonding ratio, concrete compressive strength, and strand diameter.

Test specimen design

The test specimens were designed according to the eighth edition of the AASHTO LRFD specifications.⁹ All subsequent references to the AASHTO LRFD specifications in this paper will be to the eighth edition unless otherwise noted. All applicable requirements (in particular, providing sufficient splitting resistance and confinement reinforcement and ensuring adequate longitudinal tensile resistance) were satisfied with the exception of the following:

- “The number of partially debonded strands should not exceed 25 percent of the total number of strands.”
- “The number of debonded strands in any horizontal row shall not exceed 40 percent of the strands in that row.”

The wording for the first requirement in the AASHTO LRFD specifications was nonmandatory (“should,” not “shall”), and the commentary indicated that a greater

percentage based on “successful past practice” may be considered. Some states relax the 25% limit for certain conditions and girder shapes; for example, Texas permits up to 75% debonding. In lieu of the AASHTO debonding requirements, the following rules were followed to detail the test specimens.

- single-web flanged girders (AASHTO BT-54, AASHTO Type III, and Nebraska NU-1100)
 - Do not debond more than 50% of the bottom-row strands.
 - Keep the outermost strands in all rows located within the full-width section of the flange bonded.
 - With the exception of the outermost strands, debond strands further from the vertical centerline of the section preferentially to those nearer the centerline.
 - Use a strut-and-tie (STM) model to check capacity of transverse bulb splitting reinforcing steel based on strand geometry. The STM model has been described by Harries et al.¹⁰ and Shahrooz et al.¹
- double-web sections with bottom flanges (AASHTO BI-36 and Texas U-40)
 - Do not debond more than 50% of the bottom-row strands.
 - Debond strands from the centerline of the section outward.
 - For bearings placed below webs not connected by an end diaphragm, engage a width equal to the extension of all webs at supports.
- all girders
 - In accordance with article 5.9.4.3.3 of the AASHTO LRFD specifications, debonding terminations (that is, initiation of the strand embedment) were staggered such that no more than 40% of debonded strands and four strands were terminated at any section. Terminations were staggered 36 in. (910 mm) along the girder length. Debonded strands were distributed symmetrically about the vertical centerline of the component cross section.

The provision for greater amounts of partial debonding required additional nonprestressed longitudinal reinforcement to ensure that shear capacity near the girder ends would comply with article 5.7.3.5 of the AASHTO LRFD specifications.^{1,11} These additional longitudinal bars were provided in the form of hairpins (two longitudinal bars per unit) or standard 180-degree hooks so that they could be fully developed close to the face of the girder support.

Specimen details

Tables 1 and 2 summarize details of the specimens, including the maximum debonding ratio dr for each section, the debonding ratios for each layer of reinforcement and each termination section, and measured concrete strengths at release and at time of test. Figure 1 shows the strand patterns and placement of nonprestressed reinforcement. Except for the AASHTO BI-36 girder, all the girders had a 6 in. (150 mm) thick slab over the entire width of the top flange. The deck slab reinforcement was designed according to the empirical design procedure described in article 9.7.2.5 of the AASHTO LRFD specifications.⁹ The AASHTO BI-36 specimen was tested without a slab because it is common practice to use this section in adjacent box-girder bridges with only an asphalt deck. In addition, a 2.5 ft (0.76 m) thick end diaphragm was provided for the AASHTO BI-36 girder to replicate common practice used in box girders.

Table 3 presents the material properties for the reinforcing steel, which was ASTM A615¹² Grade 60 (414 MPa) rein-

forcement. The strands were 270 ksi (1860 MPa) low-relaxation strands.

In each girder, end B satisfied all extant requirements and guidelines of the eighth edition of the AASHTO LRFD specifications⁹ with respect to strand partial debonding. End A exceeded the recommended partial debonding limits. Nevertheless, additional nonprestressed reinforcement was required to satisfy article 5.7.3.5 in all but one case (AASHTO BI-36 end B).

Test setup

The girders were supported on 12 in. (300 mm) long neoprene pads like those typically used in bridge construction. For single-web flanged sections, full-flange-width pads, having a thickness of 1.375 in. (34.93 mm), were provided for all the girders except for the AASHTO BT-54 girder, which had only 22 in. (560 mm) of the 24.5 in. (622 mm) bottom flange width supported due to pad availability. For the AASHTO BI-36 specimen, two 9 in. (230 mm) wide by 3 in. (76 mm) thick neoprene pads were placed under each web. Two 3 in. thick

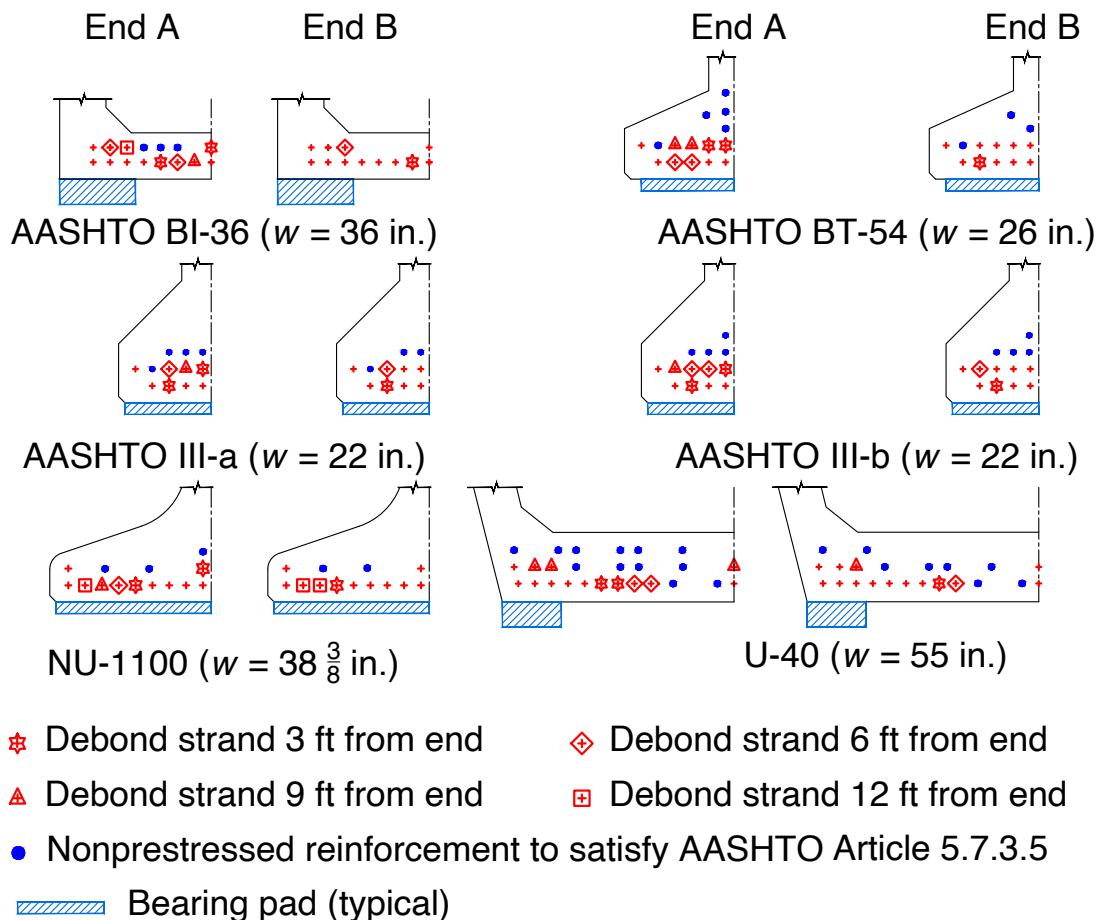


Figure 1. Debonding pattern and locations of prestressed and nonprestressed reinforcement. Note: w = width of bottom flange. 1 in. = 25.4 mm; 1 ft = 0.305 m.

Table 1. Concrete and prestressing details of the test specimens

Girder	End	f'_{ci} , ksi	f'_c at time of test, ksi	Distribution	d_b , in.	Number of strands	Debonding ratio d_r			
							0 to 3 ft	3 to 6 ft	6 to 9 ft	9 to 12 ft
AASHTO BI-36	A	7.4	12.6	Section	0.5	22	0.50*	0.36	0.18	0.09
				Row 1		15	0.40	0.27	0.13	0
				Row 2		7	0.71	0.57	0.29	0.29
	B		Section	22		0.18*	0.09	0	0	
			Row 1	15		0.13	0	0	0	
			Row 2	7		0.29	0.29	0	0	
AASHTO BT-54	A	10.2	17.4	Section	0.6	20	0.60*	0.40	0.20	0
				Row 1		10	0.40	0.40	0	0
				Row 2		10	0.80	0.40	0.40	0
	B		Section	20		0.10*	0	0	0	
			Row 1	10		0.20	0	0	0	
			Row 2	10		0.00	0	0	0	
AASHTO Type III-a	A	6.9	12.6	Section	0.5	16	0.50*	0.25	0.13	0
				Row 1		8	0.25	0	0	0
				Row 2		8	0.75	0.50	0.25	0
	B		Section	16		0.25*	0.13	0	0	
			Row 1	8		0.25	0	0	0	
			Row 2	8		0.25	0.25	0	0	
AASHTO Type III-b	A	8.3	13.8	Section	0.5	18	0.56*	0.33	0.11	0
				Row 1		8	0.25	0	0	0
				Row 2		10	0.80	0.60	0.20	0
	B		Section	18		0.22*	0.11	0	0	
			Row 1	8		0.25	0	0	0	
			Row 2	10		0.20	0.20	0	0	
Nebraska NU-1100	A	8.4	14.0	Section	0.7	22	0.45*	0.27	0.18	0.09
				Row 1		18	0.44	0.33	0.22	0.11
				Row 2		4	0.50	0	0	0
	B		Section	22		0.27*	0.18	0.18	0.18	
			Row 1	18		0.33	0.22	0.22	0.22	
			Row 2	4		0.00	0	0	0	
Texas U-40	A	6.9	12.8	Section	0.6	26	0.50*	0.35	0.19	0
				Row 1		19	0.42	0.21	0	0
				Row 2		7	0.71	0.71	0.71	0
	B		Section	26		0.23*	0.15	0.08	0	
			Row 1	19		0.21	0.11	0	0	
			Row 2	7		0.29	0.29	0.29	0	

Note: d_b = nominal strand diameter; d_r = debonding ratio; f'_c = compressive strength of concrete; f'_{ci} = compressive strength of concrete at time of initial loading or prestressing. 1 in. = 25.4 mm; 1ft = 0.305 m; 1 ksi = 6.895 MPa.

*The maximum debonding ratio d_r for each section. Other values represent debonding ration d_r for each layer of reinforcement and each termination section.

Table 2. Nonprestressed ASTM A615 Grade 60 reinforcement details of the test specimens

Girder	End	Distribution	Nonprestressed ASTM A615 Grade 60 reinforcement			
			Longitudinal		Transverse (no. 4)	
			Reinforcement	Cutoff point, ft	Web U shaped	Bottom flange
AASHTO BI-36	A	Section	Six no. 6	8.5	At 12 in. (outside of end diaphragm)	Three at 3 in., eight at 6 in., and at 12 in. to midspan
		Row 1				
		Row 2				
	B	Section	None	n/a		
		Row 1				
		Row 2				
AASHTO BT-54	A	Section	Two no. 6	6.5	Five at 3 in. and at 18 in. to midspan	Nine at 3 in., eleven at 6 in., and at 18 in. to midspan
		Row 1	Eight no. 6	13.5		
		Row 2				
	B	Section	Six no. 6	6.5		
		Row 1				
		Row 2				
AASHTO Type III-a	A	Section	Two no. 5	5.5	Four at 3 in. and at 18 in. to midspan	Four at 3 in., eleven at 6 in., and at 18 in. to midspan
		Row 1	Six no. 5	10.5		
		Row 2				
	B	Section	Two no. 5	6.5		
		Row 1	Four no. 5	9.5		
		Row 2				
AASHTO Type III-b	A	Section	Two no. 5	5.5	Four at 3 in. and at 18 in. to midspan	Four at 3 in., eleven at 6 in., and at 18 in. to midspan
		Row 1	Six no. 5	10.5		
		Row 2				
	B	Section	Four no. 5	5.5		
		Row 1	Four no. 5	9.5		
		Row 2				
Nebraska NU-1100	A	Section	Six no. 6	5.5	Four at 3 in. and at 12 in. to midspan	Four at 3 in., eleven at 6 in., and at 12 in. to midspan
		Row 1				
		Row 2				
	B	Section	Four no. 6	5.5		
		Row 1				
		Row 2				
Texas U-40	A	Section	Twenty-two no. 6	14.5	Four at 3 in., twenty-three at 4 in., and at 6 in. to midspan	Four at 3 in., twenty-three at 4 in., and at 6 in. to midspan
		Row 1				
		Row 2				
	B	Section	Sixteen no. 6	13.5		
		Row 1				
		Row 2				

Note: no. 5 = 16M; no. 6 = 19M; 1 in. = 25.4 mm; 1 ft = 0.305 m; 1 ksi = 6.895 MPa; Grade 60 = 414 MPa.

neoprene pads were also placed under each web of the Texas U-40 girder. These pads engaged the outer 7 in. (180 mm) width of the bottom flange. Displacement transducers were attached to the girder to measure the compression of pads during testing, and reported girder deflections were corrected for this movement.

The girders were tested in three-point bending using either a single 1200 kip (5300 kN) hydraulic ram or dual 300 kip (1300 kN) hydraulic rams in parallel. The location of the load was selected such that the shear span-to-depth ratio a/d_v would be greater than 2.0 to prevent direct transfer of the load to the support through arching action. All reported deflections were measured at the point of application of load. Each girder end was tested separately, with end B tested first. After testing end B, the girder was repositioned to test end A, which had a greater debonding ratio. The Texas U-40 girder was tested as a simply supported span; in all other cases, testing of each end consisted of a simple span L with a propped cantilever overhang (Fig. 2 and Table 4), isolating the other test end of the girder. To prevent cracking due to the self-weight of the cantilevered portion, an air jack was used to support the cantilevered end of the girder. The air pressure was calibrated such that the force in the jack actively compensated for the self-weight of the cantilevered portion throughout the duration of the test; thus, the girder was effectively tested as a simply supported span. Regions 1 and 2 in Fig. 2 identify locations where shear deformations were measured. The Texas U-40 girder was tested as a simply supported span because testing similar to that used for the other girders would have required a longer girder, which would have exceeded the laboratory's main crane capacity.

Table 3. Measured material properties of nonprestressed reinforcement

Girder	Bar size	f_y , ksi	f_u , ksi	ϵ_u
AASHTO BI-36	No. 3	82.1	120	0.126
	No. 4	72.7	112	0.128
	No. 6	65.4	102	0.186
AASHTO BT-54	No. 4	69.7	107	0.127
	No. 6	65.9	106	0.132
AASHTO Type III-a	No. 4	63.6	100	0.191
	No. 5	75.6	113	0.159
AASHTO Type III-b	No. 4	63.6	100	0.191
	No. 5	75.6	113	0.159
Nebraska NU-1100	No. 3	75.1	101	0.238
	No. 4	79.0	106	0.254
	No. 5	70.1	103	0.128
Texas U-40	No. 6	69.2	109	0.120
	No. 4	70.5	110	0.157
	No. 5	67.1	105	0.093
	No. 6	67.6	110	0.145

Note: f_u = ultimate strength; f_y = yield strength; ϵ_u = ultimate strain. No. 3 = 10M; no. 4 = 13M; no. 5 = 16M; no. 6 = 19M; 1 ksi = 6.895 MPa.

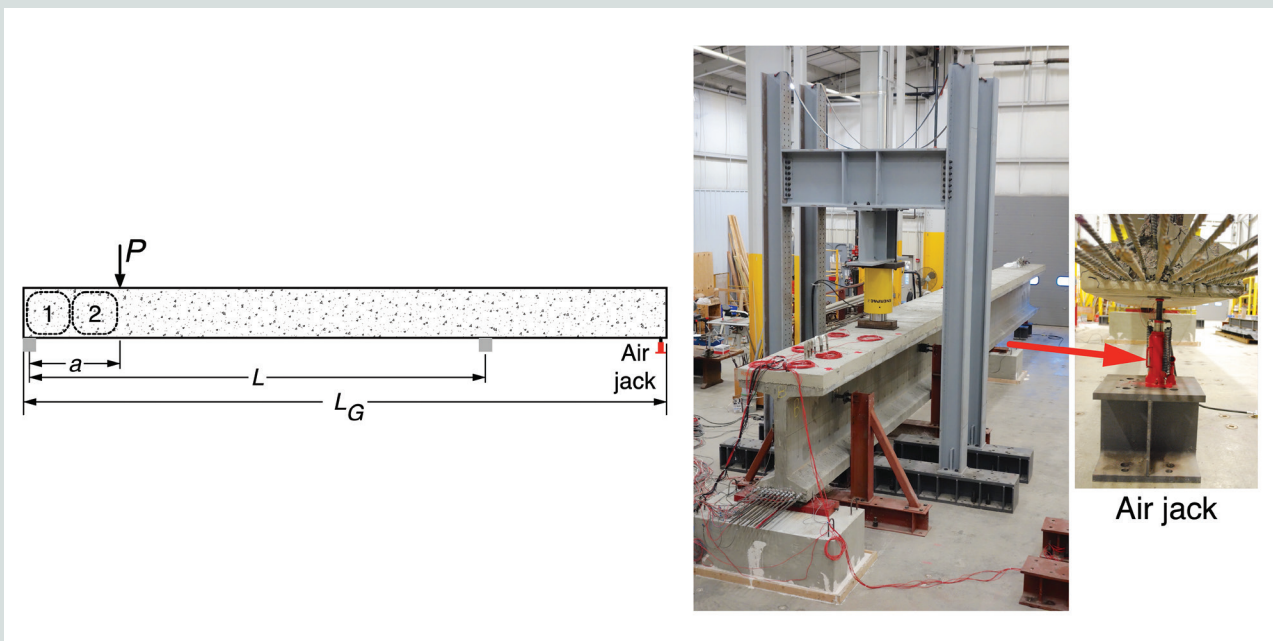


Figure 2. Test setup for test specimen AASHTO BT-54. Note: a = shear span; L = span length; L_G = overall girder length; P = load.

Test results and discussion

Except for the Nebraska NU-1100 girder and end B of the Texas U-40 girder, all specimens were loaded to failure. Failure at end B of the Texas U-40 specimen would have compromised, if not prevented, testing of end A; therefore, end B of this girder was loaded to only the capacity predicted by the AASHTO LRFD specifications. It was deemed unsafe to load the Nebraska NU-1100 girder, which had twenty-two 0.7 in. (18 mm) diameter strands, to failure given the amount of energy that would have been released in the event of a sudden failure. Therefore, this girder was loaded to only slightly above its predicted capacity.

Capacity, stiffness, and failure mode

Figure 3 shows the failure patterns of the girders in which both ends were loaded to their ultimate capacities. Based on these photographs, the failure modes were characterized as indicated in the figures. In general, comparing end A and end B of the same girder demonstrated that the failure modes were not influenced by the amount of debonding. End A of the Texas U-40 girder failed due to a combination of shear tension and bearing (Fig. 3).

The measured material properties were used to calculate the expected capacity of each specimen per the AASHTO LRFD specifications (referred to herein as the AASHTO-predicted capacity). For capacity calculations, the experimental loading conditions were used (single-point loading) and all failure modes were considered. In all but one case, shear was found to be the controlling mode; however, end B of the AASHTO BI-36 specimen was controlled by the available tensile capacity at the inside face of the support. In the calculations, resistance factors were taken as unity because the test girders were cast under controlled conditions, the loading was well defined and known from theoretical deduction, and the purpose of the calculation was to determine a predicted capacity and not a design load. The measured applied loads (and shears) were normalized with respect to the calculated capacities of each girder. The measured deflections at the point of loading were normalized with respect to the deflection measured at the predicted capacity. **Figure 4** shows the resulting normalized load-deflection responses. In each case, end B met the extant limits on the amount of debonding from the AASHTO LRFD specifications,⁹ whereas end A exceeded these limits.

All specimens successfully developed their predicted capacities. The failure loads were at least 50% greater than the AASHTO-predicted capacities (without reduction factors) calculated using measured material properties. Moreover, at peak load, which corresponded to failure if the specimen was loaded to its ultimate capacity, the deflection was at least 2.3 times that when the predicted capacity was developed. The large amounts of debonding present in the end A tests did not affect the expected load-carrying or displacement capacity (ductility).

For the AASHTO Type III-a and Type III-b girders, the normalized deflections at peak load for end A and end B were

Table 4. Test specimen span and location of applied load

Girder	L_g , ft	L , ft	a , ft	a/d_v
AASHTO BI-36	40	29	5	2.73
AASHTO BT-54	55	34	10	2.34
AASHTO Type III-a	55	39	7.75	2.15
AASHTO Type III-b	55	39	7.75	2.16
Nebraska NU-1100	55	39	7.75	2.20
Texas U-40	32	31	7.75	2.39

Note: a = shear span; d_v = effective shear depth; L = span length; L_g = overall girder length. 1 ft = 0.305 m.

comparable. The normalized load-deflection for the AASHTO BI-36 girder (Fig. 4) clearly illustrates that end A achieved its peak capacity at a larger deflection than end B. **Figure 5** indicates that the strands in end B of the AASHTO BI-36 girder experienced a sudden dramatic slip after achieving the peak normalized load of 1.60. End B of this specimen did not have any nonprestressed reinforcement to compensate for the reduction of prestressing force due to slip. As a result, load-carrying capacity at this end began to drop once the strands slipped (Fig. 5). The two ends of the AASHTO BT-54 girder experienced different failure modes (shear compression and sliding shear), which may explain why the normalized deflections at peak load differed between the ends of these two girders. The two ends of the Nebraska NU-1100 and Texas U-40 specimens could not be compared because in both girders, end B was not tested to failure.

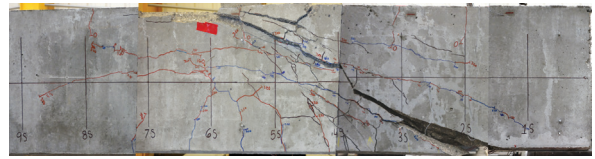
For all girders, the slopes of the normalized load-deflection relationships at end A and end B are essentially the same up to the predicted capacities (that is, when the value of normalized load is equal to 1). The larger amount of debonding at end A did not have a noticeable effect on the overall stiffness of the girders. This observation should be expected because the relatively small area of prestressing reinforcement does not affect the stiffness, and debonding, which is localized near the girder ends, has little effect on deflection.

Shear deformation

Using diagonal displacement transducers mounted to the specimen webs, the average shear deformations in two adjacent regions were obtained (Fig. 2). Region 1 is approximately one-half the shear span closer to the support, and region 2 is the other half of the shear span closer to the applied load. **Table 5** compares the average shear strains at AASHTO-predicted capacity in these regions.

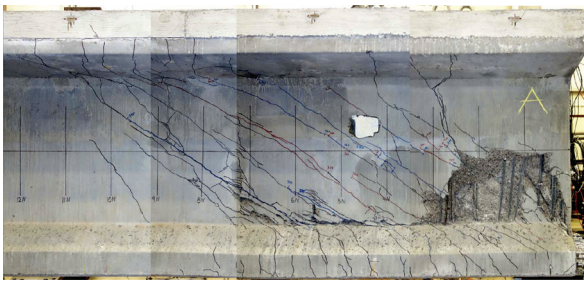


Failure mode: shear compression
End A ($dr = 0.50$)



Failure mode: shear compression
End B ($dr = 0.18$)

AASHTO BI-36

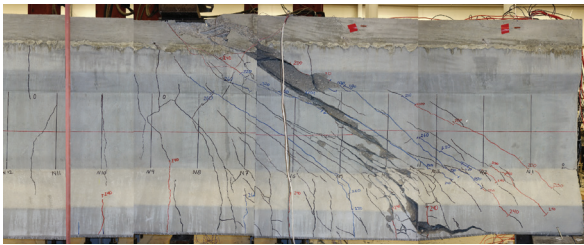


Failure mode: shear compression
End A ($dr = 0.60$)

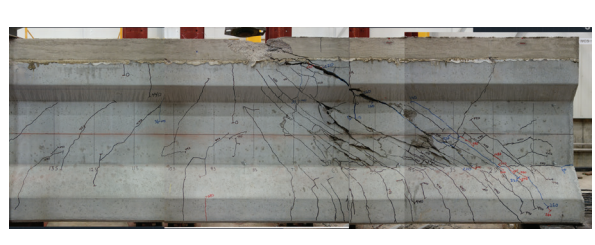


Failure mode: sliding shear at web-flange interface
End B ($dr = 0.10$)

AASHTO BT-54



Failure mode: shear compression
End A ($dr = 0.50$)

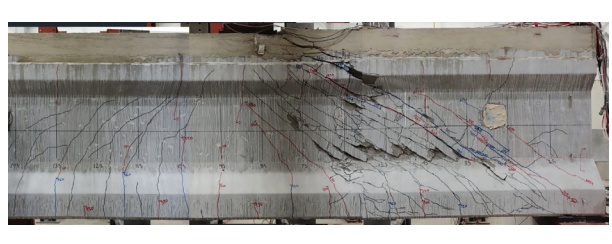


Failure mode: shear compression
End B ($dr = 0.25$)

AASHTO Type III-a

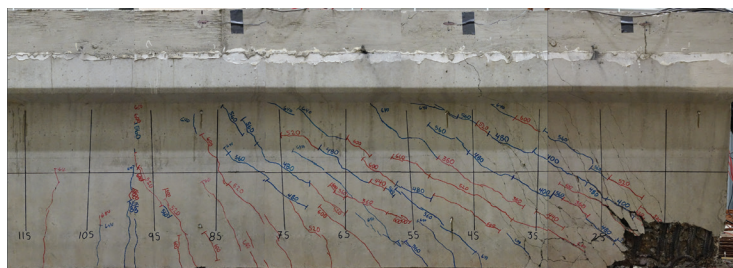


Failure mode: shear compression
End A ($dr = 0.56$)



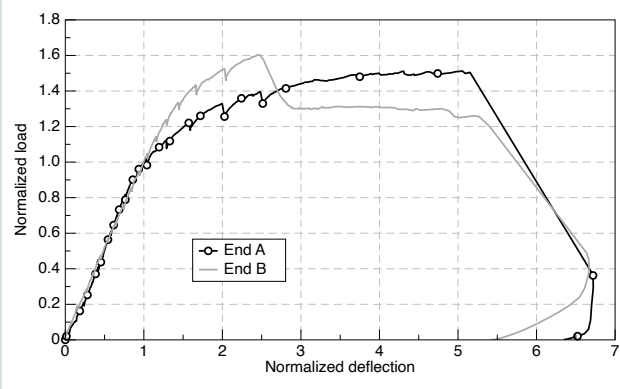
Failure mode: shear compression
End B ($dr = 0.22$)

AASHTO Type III-b

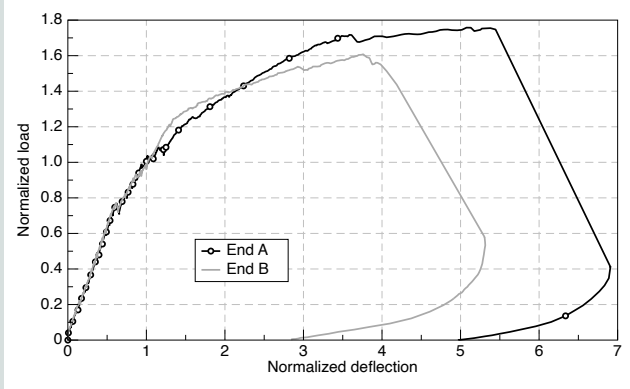


Failure mode: Shear tension and bearing
End B ($dr = 0.50$)

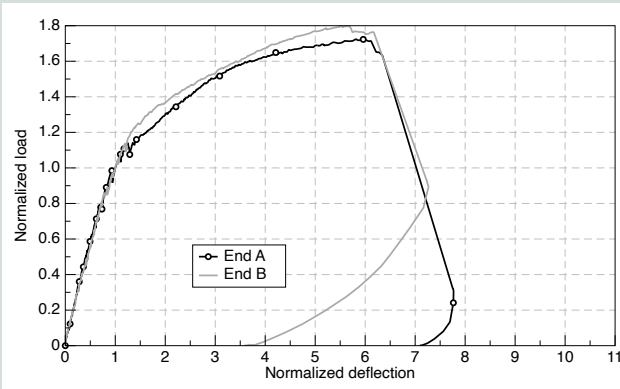
Figure 3. Crack patterns and modes of failure (compound image from multiple photos). Note: dr = debonding ratio.



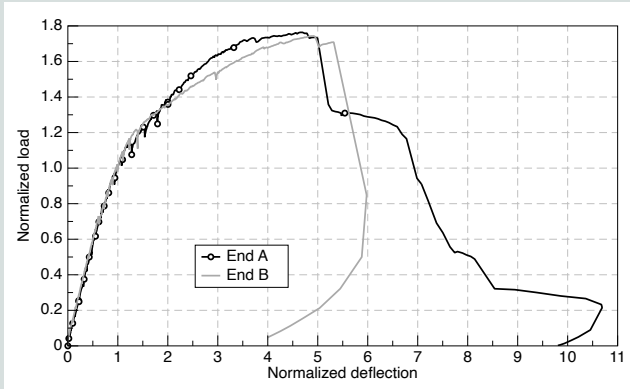
AASHTO BI-36



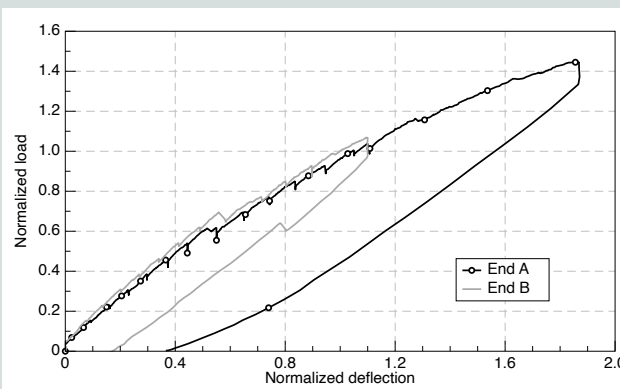
AASHTO BT-54



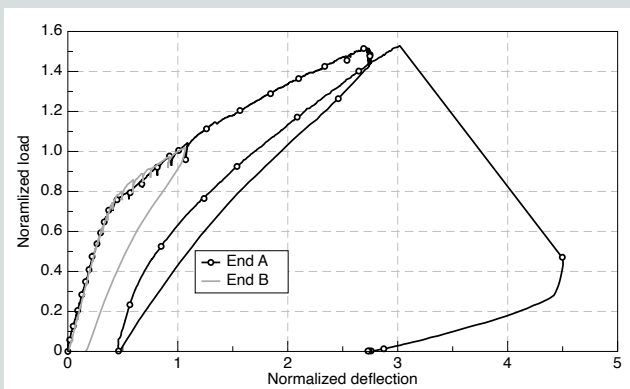
AASHTO Type III-a



AASHTO Type III-b



Nebraska NU-1100



Texas U-40

Figure 4. Normalized load-deflection responses.

In general, the shear strain at end A was larger than that at end B; on average, the strain at end A was 17% and 5% larger for region 1 and 5% larger for region 2. It is theorized that the smaller amount of prestressing force (resulting from the larger debonding ratio) at end A could not restrain the growth and widening of the cracks to the same extent as the larger amount of prestressing force at end B, and, hence, the shear strains were larger at end A.

Crack angles and widths

Photos (Fig. 3) of each girder at failure were used to determine the angles of diagonal cracks and to compare crack

patterns. The photos generally do not suggest any discernable differences between the crack patterns at the two ends of a given girder. However, for some girders (such as the AASHTO Type III-a and Type III-b specimens), end A experienced more cracking and exhibited more of a flexure-shear behavior than end B, where behavior was predominantly controlled by web shear. These observations are consistent with the smaller amount of prestressing force (due to greater debonding) at end A.

For a single girder, the average crack angles θ_{cr} (measured from horizontal) were essentially the same for the two ends

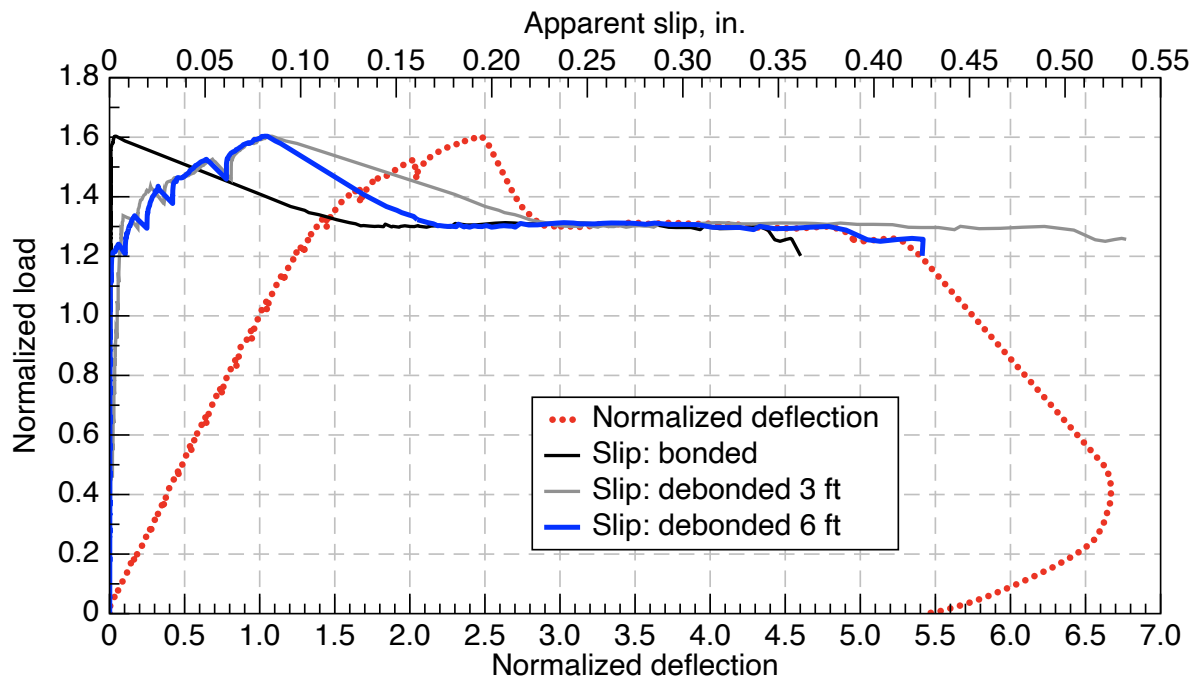


Figure 5. Normalized load versus normalized deflection and apparent strand slip for end B in test specimen AASHTO BI-36. Note: 1 in. = 25.4 mm; 1 ft = 0.305 m.

with different debonding ratios (Table 6). The maximum crack widths w_{max} at end A, which had a larger debonding ratio than end B, were generally wider than those at end B. However, the maximum measured crack widths corresponding to the AASHTO-predicted capacities were less than 0.03 in. (0.76 mm) in all cases. The larger debonding ratio did not have a deleterious effect on the observed crack angles or crack widths. Table 5 also presents the load at which the first crack occurred $P_{@1stcrack}$ normalized with respect to the AASHTO-predicted capacities P_{AASHTO} for each end of the six girders. End A cracked at a load that was, on average, 6% lower than that for end B. This observation is consistent with smaller amount of prestressing force at end A, which had a higher level of debonding than end B.

Shear resistance from transverse reinforcement

Stress-strain relationships from materials testing were used to infer stresses in the transverse reinforcement from transverse reinforcing bar strains measured in the girder tests.^{1,11} In this manner, the shear resistance provided by the transverse reinforcement V_s can be determined using Eq. (1), which is Eq. (5.7.3.3-4) of the AASHTO LRFD specifications for a case in which transverse reinforcement is perpendicular to the longitudinal axis and the yield strength of the transverse reinforcement f_y is substituted with the inferred stress f_v :

$$V_s = \frac{A_v f_v d_v (\cot \theta)}{s} \quad (1) \quad f_v = \text{stress in shear reinforcement}$$

Table 5. Average shear strain at capacity predicted by the American Association of State Highway and Transportation Officials' AASHTO LRFD Bridge Design Specifications

Girder	End A		End B	
	Region 1	Region 2	Region 1	Region 2
AASHTO BI-36	0.00042	0.00068	0.00016	0.00048
AASHTO BT-54	0.00090	0.00052	n/a	n/a
AASHTO Type III-a	0.00113	0.00181	0.00068	0.00067
AASHTO Type III-b	0.00104	0.00065	0.00106	0.00100
Nebraska NU-1100	0.00142	0.00044	0.00143	0.00089
Texas U-40	0.00085	0.00125	0.00069	0.00119

Note: n/a = not applicable (because instruments had been removed).

where

A_v = area of shear reinforcement

f_v = stress in shear reinforcement

Table 6. Average measured angles and widths of cracks at capacity predicted by the American Association of State Highway and Transportation Officials' AASHTO LRFD Bridge Design Specifications

Girder	End A			End B		
	θ_{cr} , deg	w_{max} , in.	$P_{@1stcrack}/P_{AASHTO}$	θ_{cr} , deg	w_{max} , in.	$P_{@1stcrack}/P_{AASHTO}$
AASHTO BI-36	29	≤0.01	0.61	30	≤0.01	0.67
AASHTO BT-54	34	0.025	0.77	32	0.022	0.78
AASHTO Type III-a	35	0.028	0.80	35	0.014	0.89
AASHTO Type III-b	33	0.015	0.79	34	0.025	0.73
Nebraska NU-1100	32	≤0.01	0.62	32	0.015	0.70
Texas U-40	32	0.014	0.55	34	≤0.01	0.63

Note: $P_{@1stcrack}$ = load at which the first crack occurred; P_{AASHTO} = load at capacity predicted by the AASHTO LRFD specifications; w_{max} = maximum crack width; θ_{cr} = average crack angle measured from horizontal. 1 in. = 25.4 mm.

d_v = effective shear depth

θ = angle of inclination of diagonal compressive stresses

s = average spacing of shear reinforcement

The values of θ_{cr} in Table 5 were substituted for θ in the V_s calculations. This calculation was performed at six locations (every 1 ft [0.3 m] up to 6 ft [1.8 m] from the ends of the girder) where the transverse reinforcement had been instrumented. Because there was no harped prestressing strand component, the difference between the applied shear and the average of V_s from these six locations was the experimentally inferred concrete contribution to shear V_c . The value of V_c was also determined based on Eq. (5.7.3.3-3) of the AASHTO LRFD specifications. Both the experimental and calculated values of V_c were normalized by $\sqrt{f'_c b_v d_v}$.

Figure 6 plots the difference between the normalized values of V_c at end A and end B versus the difference between the level of debonding ratio at the two ends. As expected, the value of V_c at end A, which had a larger debonding ratio, was smaller than its counterpart at end B, which had a smaller debonding ratio. Thus, the beneficial effect of precompression on the concrete contribution to shear capacity is evident. AASHTO Eq. (5.7.3.3-3) indicates a similar rate of reduction compared with the test data (Fig. 6).

Apparent strand slip

For each specimen, several bonded strands and all debonded strands were instrumented with displacement transducers to measure the movements of the strands relative to the end face of the girder. For fully bonded strands, this movement is the actual slip. In the case of debonded strands, the measured slip is affected by the length of partial debonding but in a manner that cannot be corrected.

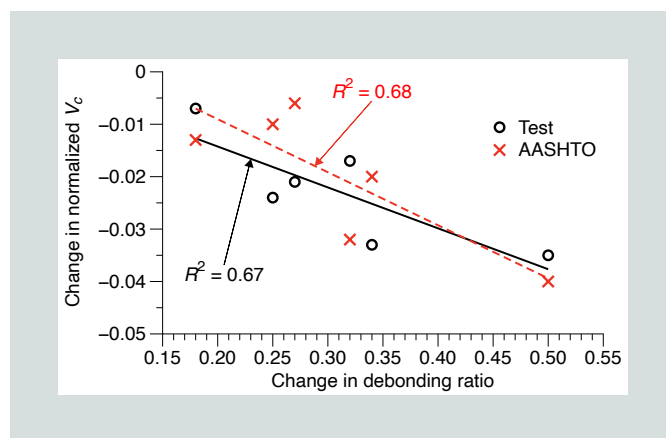


Figure 6. Normalized V_c at end A minus V_c at end B versus differences in the debonding ratios. Note: R^2 = coefficient of determination; V_c = nominal shear resistance provided by tensile stresses in the concrete.

Figure 7 compares the measured slip data at AASHTO-predicted capacities for end A and end B. The slip of bonded strands was 0.004 in. (0.1 mm) or less for all cases except for end A of the Texas U-40 girder, which experienced a slip of 0.011 in. (0.28 mm). The measured slip of debonded strands rarely exceeded 0.043 in. (1.1 mm), except for the following cases in the Texas U-40 girder:

- strands debonded 3 ft (0.9 m) at end B with slip of 0.060 in. (1.5 mm)
- end A with a debonding length of 6 ft (1.8 m) with slip of 0.073 in. (1.9 mm)
- both end A and end B in which the strands were debonded for 9 ft (2.7 m) with slips of 0.060 and 0.099 in. (1.5 and 2.5 mm), respectively

The partially debonded strands exhibited greater slip at end A than at end B, except for the debonding lengths of 12 ft

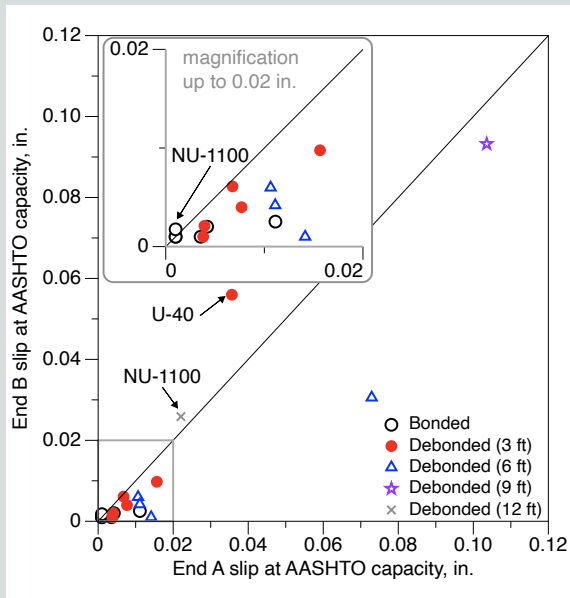


Figure 7. Comparison of slips at the capacity predicted by the American Association of State Highway and Transportation Officials' AASHTO LRFD Bridge Design Specifications. Note: 1 in. = 25.4 mm; 1 ft = 0.305 m.

(3.7 m) in the Nebraska NU-1100 girder and 3 ft (0.9 m) in the Texas U-40 girder.

The amount of debonding affected the onset of slip of bonded and debonded strands. To illustrate this dependency, **Fig. 8** compares the normalized shears corresponding to 0.01 in. (0.25 mm) slip at end A and end B. This value, which is one-tenth of the slip used for strand evaluation according to ASTM A1081,¹³ was arbitrarily selected, and similar observations can be made for other values of slip displacement. The normalized shears required to develop 0.01 in. slip for the bonded and debonded strands at end B were higher than their counterparts in end A. That is, slippage of strands in the cases with greater levels of debonding occurred sooner than in those cases with less debonding.

Contribution of longitudinal reinforcement

As part of design of the test specimens, the amounts of nonprestressed longitudinal reinforcement required at the critical section and at the interior face of the support were determined according to AASHTO Eq. (5.7.3.5-1) and (5.7.3.5-2), respectively:

$$A_{ps}f_{ps} + A_s f_y \geq \frac{|M_u|}{d_v \phi_f} + 0.5 \frac{N_u}{\phi_c} + \left(\left| \frac{V_u}{\phi_v} - V_p \right| - 0.5V_s \right) \cot \theta \quad (\text{AASHTO 5.7.3.5-1})$$

where

A_s = area of nonprestressed tension reinforcement

M_u = applied factored bending moment at the section under consideration

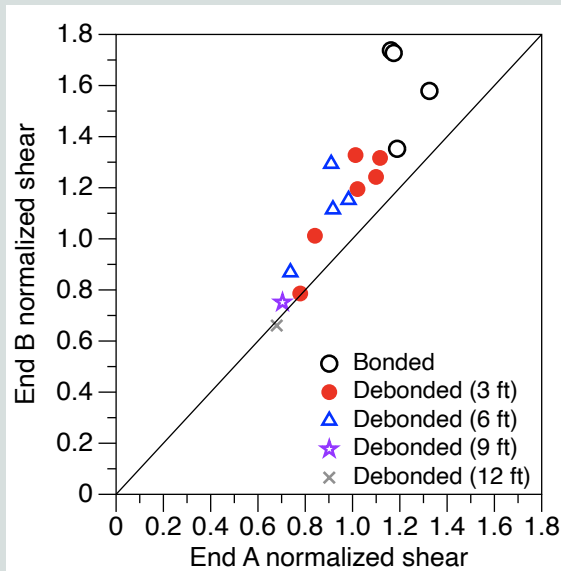


Figure 8. Comparison of normalized shear corresponding to 0.01 in. slip. Note: 1 in. = 25.4 mm; 1 ft = 0.305 m.

ϕ_f = resistance factor for moment resistance

N_u = applied factored axial force at the section under consideration, taken as positive if tensile

ϕ_c = resistance factor for axial resistance

V_u = applied factored shear force at section

ϕ_v = resistance factor for shear resistance

V_p = component in the direction of the applied shear of the effective prestressing force

θ = angle of inclination of diagonal compressive stresses

$$A_{ps}f_{ps} + A_s f_y \geq \left(\frac{V_u}{\phi_v} - 0.5V_s - V_p \right) \cot \theta \quad (\text{AASHTO 5.7.3.5-2})$$

Based on a similar procedure used to calculate shear resistance from transverse reinforcement, stresses in the nonprestressed longitudinal reinforcement were inferred from the experimentally determined stress-strain relationships.^{1,11} **Table 7** presents the resulting nonprestressed reinforcement stresses f_s normalized with respect to their measured yield strengths for the AASHTO-predicted capacity and at the maximum experimentally applied load. If available, stresses at three sections are given at the critical section near the support (XS2), a distance d_v from the interior face of the support (XS3), and at the point where the load was applied (XS4).

At the AASHTO-predicted capacity, the stress in the nonprestressed reinforcing steel is equal to or less than

Table 7. Normalized stress in nonprestressed longitudinal reinforcement

Girder	At AASHTO-predicted capacity						At maximum load					
	End A			End B			End A			End B		
	f_s/f_y			f_s/f_y			f_s/f_y			f_s/f_y		
	XS2	XS3	XS4	XS2	XS3	XS4	XS2	XS3	XS4	XS2	XS3	XS4
AASHTO BI-36	0.024	0.094	0.173	n/a	n/a	n/a	1.02	1.11	0.89	n/a	n/a	n/a
AASHTO BT-54	0.037	0.065	0.124	0.12	0.14	n/a	1.01	1.02	0.45	1.02	0.76	n/a
AASHTO Type III-a	0.104	0.127	0.148	0.04	0.11	0.16	0.77	1.08	0.97	0.67	0.99	0.96
AASHTO Type III-b	0.051	0.130	0.163	0.18	0.07	0.03	1.03	1.04	0.94	0.86	0.90	0.71
Nebraska NU-1100	0.261	0.074	n/a	0.24	0.08	n/a	0.79	0.17	n/a	0.31	0.09	n/a
Texas U-40	0.350	0.281	n/a	0.29	0.15	n/a	0.99	0.93	n/a	0.30	0.19	n/a

Note: d_v = effective shear depth; f_s = nonprestressed reinforcement stresses; f_y = yield strength of reinforcing bar; n/a = not applicable; XS2 = critical section near support; XS3 = section a distance d_v from the interior face of support; XS4 = point of load application.

$0.35f_y$; however, the longitudinal nonprestressed reinforcement is assumed to have yielded according to AASHTO Eq. (5.7.3.5-1) and (5.7.3.5-2). A plausible explanation for this difference is that AASHTO LRFD specifications do not account for the tensile strength of the precompressed concrete. Hence, the available capacity is greater than the predicted $A_{ps}f_{ps} + A_s f_y$ term.

The results in Table 7 indicate that normalized nonprestressed longitudinal reinforcement stresses at end A were generally larger than those at end B. This observation is consistent with the differences in the amount of prestressing force at the two ends resulting from partial debonding. The smaller prestressing force at end A resulted in more cracking and, hence, an earlier onset and higher redistribution of the tensile force from the precompressed concrete to the reinforcement. For most of the girders that were loaded to failure, the nonprestressed longitudinal bars began to yield at either section XS2 (the critical section near the support) or section XS3 (the section at the distance d_v from the interior face of the support), or at both sections. All nonprestressed reinforcement was fully developed at these locations using hairpins or standard hooks.

Conclusion

Experimental testing of six full-sized girders was conducted to examine the effects of debonding on girder performance. The main test variables were girder shape, debonding ratio, concrete strength, and strand diameter. Each girder end was tested separately, with end A having a greater debonding ratio than end B. Detailing and loading of the two girder ends were identical with the exception of the debonding ratios. Girders were designed to meet all requirements set forth in the eighth edition of the AASHTO LRFD specifications except for the 25% limit on debonding ratios. Based on the presented experimental results, the following conclusions are made:

- The experimentally determined girder capacities were in excess of those computed based on the AASHTO LRFD specifications using measured material properties and prestress losses with no strength reduction factor. The large amounts of debonding at end A were not detrimental to the load-carrying capacity of the girders.
- Regardless of the debonding ratios, the measured deflection at the peak load was several times larger than the measured deflection at the capacity calculated using the AASHTO LRFD specifications, which indicates adequate performance in terms of displacement capacity (ductility).
- Up to the AASHTO-predicted capacity, the slopes of the normalized load-deflection curves were nearly identical for end A and end B. The larger debonding ratio at end A did not have a noticeable impact on normalized girder stiffness.
- In general, the average measured concrete shear strain for a given value of applied shear was larger at end A than at end B. This observation should be expected because the smaller amount of prestressing force (resulting from the larger debonding ratio) at end A would not restrain the growth and widening of the cracks to the same extent as in end B.
- The crack widths at end A (larger debonding ratio) were in general slightly wider than those at end B, the maximum measured crack widths corresponding to the AASHTO-predicted capacities were small regardless of the debonding ratio, and the largest recorded crack width was less than 0.03 in. (0.76 mm). Moreover, for a single girder, the average crack angles were essentially the same for the two ends with different debonding ratios. The larger debonding ratio did not have a deleterious effect on observed crack angles or crack widths.

- The smaller prestressing force at end A resulted in more cracking, and, hence, the contribution of the concrete to the shear resistance was reduced. However, the performance was not adversely affected because shear equations in the AASHTO LRFD specifications capture the smaller concrete shear strength as the level of debonding increases.
- In general, there were no discernable differences between the crack patterns at the ends of a given girder. However, for some girders (such as AASHTO Type III-a and Type III-b), end A experienced more cracking and exhibited more of a flexure-shear behavior than end B, whose behavior was predominantly controlled by web shear. These observations are consistent with the smaller amount of prestressing force (due to greater debonding) at end A.
- At AASHTO-predicted girder capacities, measured slip did not exceed 0.03 in. (0.76 mm), except in the debonded strands in the Texas U-40 specimen, which slipped between 0.036 and 0.104 in. (0.91 and 2.64 mm). The measured slip of fully bonded strands was negligible in all cases. All girders exhibited acceptable amounts of strand slip up to the capacity required in the AASHTO LRFD specifications.
- The nonprestressed reinforcement used to compensate for larger debonding ratios was found to be adequate in terms of capacity. Although this reinforcement could not replicate the effects of prestressing force in bonded strands, investigators found only small differences in the overall stiffness, crack widths, and crack patterns and angles of cracks of the two girder ends with different magnitudes of debonding ratios. The results are consistent with the hypothesis that bonded strand and nonprestressed tension reinforcement work together to resist longitudinal forces induced by shear (that is, those calculated using Eq. [5.7.3.5-1] and [5.7.3.5-2] of the AASHTO LRFD specifications).

AASHTO and the American Society of Civil Engineers have addition resources that cover related topics.¹⁴⁻¹⁸

Ninth edition of the AASHTO LRFD specifications updates

The reported research was conducted as part of NCHRP project 12-91, “Strand Debonding for Pretensioned Girders.” The results of this research program¹ along with previous studies³⁻⁸ were used to update the requirements for debonded strands in the ninth edition of the AASHTO LRFD specifications. Following are differences between the revised AASHTO article 5.9.4.3.3 and the experimental program:

- The ninth edition of the AASHTO LRFD specifications limits the number of debonded strands per row to 45% of the strands in that row unless approved by the owner. This revised requirement was exceeded at end A of all

specimens. Up to 80% of strands per row were debonded in the test girders.

- The AASHTO limit of 45% debonded strands per row also means that the total number of debonded strands is limited to 45%. In the test girders, overall debonding ranged from 10% to 60% of the total strands in the cross section.
- The AASHTO LRFD specifications require that the debonding termination locations be at least $60d_b$, where d_b is the nominal strand diameter. A longitudinal spacing of debonding termination locations of 36 in. (910 mm) was used in the test specimens. For 0.5 and 0.6 in. (13 and 15 mm) diameter strands, this spacing corresponds to $72d_b$ and $60d_b$, respectively; thus, this requirement was met by all test specimens except the Nebraska NU-1100 girder. For the NU-1100 girder, which had 0.7 in. (18 mm) diameter strands, the spacing corresponded to $51.4d_b$.
- The AASHTO LRFD specifications require that the locations of bonded and debonded strands be alternated both horizontally and vertically. This requirement was exceeded in the reported research. Many of the test specimens had adjacent strands debonded horizontally, vertically, or in both directions.
- The AASHTO LRFD specifications limit the debonding length, measured from the girder end, for simple-span girders to the smaller of 20% of the span length or one-half the span length minus the development length. This requirement was not satisfied in the test program. To accommodate practical requirements for laboratory testing, all of the girders tested had relatively short spans.
- For single-web flanged sections such as I-beams and bulb tees, the AASHTO LRFD specifications require the following. The single-web flange test specimens (Nebraska NU-1100, AASHTO Type III, and AASHTO BT-54) met the last requirement but did not meet the first two requirements. Instead, an STM model^{1,10} was used to check the capacity of the confining reinforcement.
 - All strands within the horizontal limits of the web must remain bonded if the total number of debonded strands exceeds 25%.
 - All strands within all rows that are within the projected width of the flange must be bonded.
 - The strands that are the farthest from the vertical centerline must be debonded.
- For box beams, U girders, or voided slabs, the AASHTO LRFD specifications require the following. The multi-web flange test specimens (AASHTO BI-36 and Texas

U-40) met the last requirement but did not meet the first two requirements.

- Debonded strands must be distributed uniformly between the webs.
- Strands must be bonded within 1.0 times the web-width projection.
- The outermost strands must be bonded.

Although the test specimens did not meet most of the revised requirements in the ninth edition of the AASHTO LRFD specifications, the performance of the test girders was found to be adequate. In conclusion, the experimental results demonstrate that the changes to the AASHTO LRFD specifications are supported and continue to be conservative.

Acknowledgments

The research presented in this paper was a part of NCHRP project 12-91, “Strand Debonding for Pretensioned Girders.” The authors wish to thank the NCHRP Project Panel and the senior program officer, Waseem Dekelbab, for their project oversight and valuable insight and feedback throughout the project. Malory Gooding, a student at the University of Cincinnati, and James Thompson, a student at Cincinnati State Technical and Community College working through a cooperative education program with the University of Cincinnati, were instrumental in the experimental phase, and their contributions are gratefully acknowledged.

References

1. Shahrooz, B. M., R. A. Miller, K. A. Harries, Q. Yu, and H. G. Russell. 2017. *Strand Debonding for Pretensioned Girders*. NCHRP (National Cooperative Highway Research Program) report 849. Washington, DC: Transportation Research Board, National Research Council.
2. AASHTO (American Association of State Highway and Transportation Officials). 2020. *AASHTO LRFD Bridge Design Specifications*, 9th ed. Washington, DC: AASHTO.
3. Shahawy, M., and B. de V Batchelor. 1991. *Bond and Shear Behavior of Prestressed AASHTO Type II Beams*. Progress report. Tallahassee, FL: Structural Research Center, Florida Department of Transportation.
4. Shahawy, M., B. Robinson, and B. de V. Batchelor. 1993. *An Investigation of Shear Strength of Prestressed Concrete AASHTO Type II Girders*. Research report. Tallahassee, FL: Structures Research Center, Florida Department of Transportation.
5. Russell, B. W., N. H. Burns, and L. G. ZumBrunnen. 1994. “Predicting the Bond Behavior of Prestressed Concrete Beams Containing Debonded Strands.” *PCI Journal* 39 (5): 60–77.
6. Russell, B. W., and N. H. Burns. 1994. “Fatigue Tests on Prestressed Concrete Beams Made with Debonded Strands.” *PCI Journal* 39 (6): 70–88.
7. Langefeld, D. P., and O. Bayrak. 2012. *Anchorage-Controlled Shear Capacity of Prestressed Concrete Bridge Girders*. Technical report. Austin, TX: University of Texas.
8. Hamilton, H. R., G. R. Consolazio, and B. E. Ross. 2013. *End Region Detailing of Pretensioned Concrete Bridge Girders: Final Report*. Tallahassee, FL: Florida Department of Transportation.
9. AASHTO. 2017. *AASHTO LRFD Bridge Design Specifications*, 8th ed. Washington, DC: AASHTO.
10. Harries, K. A., B. M. Shahrooz, B. E. Ross, P. Ball, and H. R. Hamilton. 2019. “Modeling and Detailing Pretensioned Concrete Bridge Girder End Regions Using the Strut and Tie Approach.” *ASCE Journal of Bridge Engineering* 24 (3): 04018123. [https://doi.org/10.1061/\(ASCE\)BE.1943-5592.0001354](https://doi.org/10.1061/(ASCE)BE.1943-5592.0001354).
11. Bolduc, M. W. 2020. “Full-Scale Testing of Pretensioned Concrete Girders with Partially Debonded Strands.” PhD dissertation. University of Cincinnati, Cincinnati, OH.
12. ASTM International. 2022. *Standard Specification for Deformed and Plain Carbon-Steel Bars for Concrete Reinforcement*. ASTM A615/A615M-22. West Conshohocken, PA: ASTM International.
13. ASTM International. 2015. *Standard Test Method for Evaluating Bond of Seven-Wire Steel Prestressing Strand*. ASTM A1081/A1081M-15. West Conshohocken, PA: ASTM International.
14. AASHTO. 2012. *Standard Specification for Steel Strand, Uncoated Seven-Wire for Concrete Reinforcement*. AASHTO M 203M. Washington, DC: AASHTO.
15. AASHTO. 2014. *Standard Method of Test for Compressive Strength of Cylindrical Concrete Specimens*. AASHTO T 22. Washington, DC: AASHTO.
16. AASHTO. 2014. *Standard Method of Test for Mechanical Testing of Steel Products*. AASHTO T 244. Washington, DC: AASHTO.
17. AASHTO. 2016. *AASHTO LRFD Bridge Design Specifications*, 7th ed., with 2015 and 2016 interim revisions. Washington, DC: AASHTO.
18. Bolduc, M. W., A. Gaur, B. M. Shahrooz, K. A. Harries, R. A. Miller, and H. G. Russell, H.G. 2020. “Evaluation

of Pretensioned Girders with Partial Strand Debonding.” *ASCE Journal of Bridge Engineering* 25 (8). [https://doi.org/10.1061/\(ASCE\)BE.1943-5592.0001585](https://doi.org/10.1061/(ASCE)BE.1943-5592.0001585).

Notation

a	= shear span	V_p	= component in the direction of the applied shear of the effective prestressing force
A_{ps}	= area of prestressing steel	V_s	= shear resistance provided by shear reinforcement
A_s	= area of nonprestressed tension reinforcement	V_u	= applied factored shear force at section
A_v	= area of shear reinforcement	w	= width of bottom flange
dr	= debonding ratio	w_{max}	= maximum crack width
d_b	= nominal strand diameter	ϵ_u	= ultimate strain of nonprestressed reinforcement
d_v	= effective shear depth	θ	= angle of inclination of diagonal compressive stresses
f'_c	= compressive strength of concrete	θ_{cr}	= average crack angle measured from horizontal
f'_{ci}	= compressive strength of concrete at time of initial loading or prestressing	ϕ_c	= resistance factor for axial resistance
f_{ps}	= average stress in prestressing steel at nominal flexural resistance	ϕ_f	= resistance factor for moment resistance
f_s	= nonprestressed reinforcement stresses	ϕ_v	= resistance factor for shear resistance
f_v	= stress in shear reinforcement		
f_y	= yield strength of nonprestressed reinforcement		
h	= overall depth of a component		
L	= span length		
L_G	= overall girder length		
M_u	= applied factored bending moment at section		
N_u	= applied factored axial force at section, taken as positive if tensile		
P	= load		
$P_{@1stcrack}$	= load at which the first crack occurred		
P_{AASHTO}	= load at capacity predicted by the AASHTO LRFD specifications		
R^2	= coefficient of determination		
s	= average spacing between mild shear reinforcement		
V_c	= nominal shear resistance provided by tensile stresses in the concrete		

About the authors



Mathew W. Bolduc, PhD, PE, is a former graduate student at the University of Cincinnati in Cincinnati, Ohio.



Bahram M. Shahrooz, PhD, FACI, FASCE, FSEI, PE, is a professor of structural engineering at the University of Cincinnati.



Kent A. Harries, PhD, PEng, FASCE, FACI, FIIFC, is a professor of structural engineering and mechanics at the University of Pittsburgh in Pittsburgh, Pa.



Richard A. Miller, PhD, FPCI, PE, is a professor of civil engineering and department head at the University of Cincinnati.



Henry G. Russell, PhD, PE, is an engineering consultant who has been involved with applications of concrete for bridges for about 50 years. He is a former managing technical editor of *Aspire*, the concrete bridge magazine.



William A. Potter, PE, is the Florida state structures design engineer.

Abstract

To develop a unified approach for the design of partially debonded strands in prestressed concrete highway bridge girders, a coordinated analytical and experimental investigation was conducted. This investigation examined amounts of partial debonding,

distribution of partially debonded strands within the cross section, debonded lengths, locations and staggering of termination of debonded strands, confinement of debonded regions and their termination points, and the impact of adding nonprestressed reinforcement in the region of partial debonding. The results from testing full-scale I- and U-shaped girders indicate that partially debonding strands does not result in deleterious performance if adequate reinforcement is provided to resist the longitudinal tension due to bending and shear. Crack patterns and angles were not noticeably affected by the amount of debonding. Regardless of the debonding ratio, the maximum measured crack widths at the capacities predicted by the eighth edition of the American Association of State Highway and Transportation Officials' *AASHTO LRFD Bridge Design Specifications* remained small. The requirements for debonded strands were revised significantly in the ninth edition of the AASHTO LRFD specifications based on the presented research.

Keywords

Bridge, multiweb flange section, nonprestressed longitudinal reinforcement, partially debonded strand, prestressed concrete girder, single-web flanged section, strand debonding.

Review policy

This paper was reviewed in accordance with the Precast/Prestressed Concrete Institute's peer-review process. The Precast/Prestressed Concrete Institute is not responsible for statements made by authors of papers in *PCI Journal*. No payment is offered.

Publishing details

This paper appears in *PCI Journal* (ISSN 0887-9672) V. 68, No. 2, March–April 2023, and can be found at <https://doi.org/10.15554/pcij68.2-01>. *PCI Journal* is published bimonthly by the Precast/Prestressed Concrete Institute, 8770 W. Bryn Mawr Ave., Suite 1150, Chicago, IL 60631. Copyright © 2023, Precast/Prestressed Concrete Institute.

Reader comments

Please address any reader comments to *PCI Journal* editor-in-chief Tom Klemens at tklemens@pci.org or Precast/Prestressed Concrete Institute, c/o *PCI Journal*, 8770 W. Bryn Mawr Ave., Suite 1150, Chicago, IL 60631. 